Science Advances
AAAS

advances.sciencemag.org/cgi/content/full/6/8/eaaz1955/DC1

Supplementary Materials for

Singlet-filtered NMR spectroscopy

Salvatore Mamone*, Nasrollah Rezaei-Ghaleh, Felipe Opazo, Christian Griesinger, Stefan Glöggler*

*Corresponding author. Email: salvatore.mamone@mpibpc.mpg.de (S.M.); stefan.gloeggler@mpibpc.mpg.de (S.G.)

Published 21 February 2020, *Sci. Adv.* **6**, eaaz1955 (2020)
DOI: 10.1126/sciadv.aaz1955

This PDF file includes:

Table S3. The table reports the constants defining the nuclear spin Hamiltonian as well as the parameters used to set the gc-M2S sequence in the experiments on Aβ40 presented in Fig. 2B.
Table S4. The table reports parameters used to set the gc-M2S sequence in the experiments on mouse brains presented in Fig. 3.
Materials and methods extended
References (*41*, *42*)

Supplementary information

Theoretical considerations

In this section, the theoretical aspects of the gc-M2S sequence are discussed with more detail.

The gc-M2S sequence is shown in Figure 1. Assuming negligible relaxation effects, the sequence drives the magnetization $\rho_i = (I_{1z} + I_{2z})/2$ into the zero-quantum operator $ZQ_x = I_{1x}I_{2x} + I_{1y}I_{2y}$, which is then filtered into the singlet state operator, leading to $\rho_{T_{00}} = 2\big(I_{1x}I_{2x} + I_{1y}I_{2y} + I_{1z}I_{2z}\big)/3$ (T_{00} filter) and finally back into magnetization $\rho_f = (I_{1z} + I_{2z})/3$ plus orthogonal operators. The numeric coefficients correspond to a sequence with unitary transfer for the conversion $(I_{1z} + I_{2z})/2 \rightleftharpoons ZQ_x$ in the magnetization-to-singlet and singlet-to-magnetization blocks, respectively. The 2/3 factor originates from the T_{00} filter, which projects ZQ_x onto $T_{00} = I_{1x}I_{2x} + I_{1y}I_{2y} + I_{1z}I_{2z}$.

The full liquid state spin Hamiltonian has been introduced in equation (1). In the discussion of the sequence, the effects of the mean chemical shift Hamiltonian H_0 on the spin dynamics will be disregarded for the following reasons. Firstly, H_0 commutes with H_1 and the effects on the evolution can be discussed independently. Secondly, H_0 is refocused by the echoes used in the sequence and has no net effect at the terminal point of the SQ blocks. Finally, H_0 commutes with all the operators in the zero-quantum space of interest for the sequence, as defined in due course, which implies no net effect during the evolution in the ZQ blocks. It will also be assumed that all the pulses are ideal delta-pulses corresponding to exact nominal rotations of the spin operators. The previous arguments ensure that the magnetization-singlet-magnetization transfer is achieved in an offset independent manner.

By working the commutator between H_1

	$$H_1(\omega_\delta, J_{12}) = \omega_\delta(I_{1z} - I_{2z})/2 + 2\pi J_{12}\, I_1 \cdot I_2$$	*S(1)*

and the set of single quantum operators

	$$SQ_1 = \left\{\frac{I_{1x} + I_{2x}}{2}, I_{1y}I_{2z} + I_{1z}I_{2y}, I_{1x}I_{2z} - I_{1z}I_{2x}, \frac{I_{1y} - I_{2y}}{2}\right\}$$	*S(2)*
	$$SQ_2 = \left\{\frac{I_{1y} + I_{2y}}{2}, I_{1x}I_{2z} + I_{1z}I_{2x}, I_{1y}I_{2z} - I_{1z}I_{2y}, \frac{I_{1x} - I_{2x}}{2}\right\}$$	*S(3)*

two independent equivalent matrix blocks are obtained. By diagonalizing the Hamiltonian $H_1\tau$, where τ is given in equation (2), in the single quantum space SQ_1 and using the fact that

	$$R_\pi^\dagger H_1(\omega_\delta, J_{12}) R_\pi = -\omega_\delta(I_{1z} - I_{2z})/2 + 2\pi J_{12}\, I_1 \cdot I_2$$	*S(4)*

it possible to show that the basic echo delay $\tau - \pi - \tau - \pi$ confines the spin dynamics within the single-quantum space defined by the operators in the set SQ_1 or SQ_2 at time points multiple of 2τ.

At the end of the echo train, the evolution is described by the tensor product of 2-dimensional rotations:

$$\left[U_{SQ}^{echo}(2\tau)\right]^{n_1} = R(n_1\theta_1)\otimes R(n_1\varphi_1) = \begin{pmatrix}\mathrm{Cos}\, n_1\theta_1 & -\mathrm{Sin}\, n_1\theta_1\\ \mathrm{Sin}\, n_1\theta_1 & \mathrm{Cos}\, n_1\theta_1\end{pmatrix}\otimes\begin{pmatrix}\mathrm{Cos}\, n_1\varphi_1 & \mathrm{Sin}\, n_1\varphi_1\\ \mathrm{Sin}\, n_1\varphi_1 & \mathrm{Cos}\, n_1\varphi_1\end{pmatrix} \quad S(5)$$

where

$$\theta_1 = 2\,\mathrm{ArcTan}\left(\frac{1}{\varepsilon}\right), \quad S(6)$$

$$\varphi_1 = \pi\,\rho\,S\mathrm{ign}(J_{12}) \quad S(7)$$

Assuming that the initial operator is $\frac{I_{1x}+I_{2x}}{2}$, the echo train will lead to the operator in equation

$$\left(\frac{I_{1x}+I_{2x}}{2}\right)\xrightarrow{\left[U_{SQ}^{echo}(2\tau)\right]^{n_1}}\left(\frac{I_{1x}+I_{2x}}{2}\right)\mathrm{Cos}\, n_1\theta_1\,\mathrm{Cos}\, n_1\varphi_1 + \left(I_{1y}I_{2z}+I_{1z}I_{2y}\right)\mathrm{Cos}\, n_1\theta_1\,\mathrm{Sin}\, n_1\varphi_1 + \left(I_{1x}I_{2z}-I_{1z}I_{2x}\right)\mathrm{Sin}\, n_1\theta_1\,\mathrm{Cos}\, n_1\varphi_1 + \left(\frac{I_{1y}-I_{2y}}{2}\right)\mathrm{Sin}\, n_1\theta_1\,\mathrm{Sin}\, n_1\varphi_1 \quad S(8)$$

The useful fraction of the evolved operator that is amenable to singlet conversion is defined by $f_{SQ}^{M2S}(n_1) = |\mathrm{Sin}(n_1\theta_1)|$. Indeed, in the M2S$_{SQ}$ block, the $(\pi/2)_{\phi_2}$ pulse, where the phase ϕ_2 *is* in quadrature with that of the first pulse, brings the operator on right side of equation S(8) into the zero-quantum space comprising the operators $\left\{I_{1y}I_{2x}-I_{1x}I_{2y}, \frac{I_{1z}-I_{2z}}{2}\right\}$ and into other orthogonal spaces. The aim of the M2S$_{SQ}$ block is to maximizef_{SQ}^{M2S} by setting an appropriate number of echoes n_1. Here, we notice that a) the maximal conversion $f_{SQ}^{M2S}=1$ can be obtained only for even integer values $\pi/\theta_1 = 2k$ using $\bar{n}_1 = k$ echoes; b) for odd $\pi/\theta_1 = 2k+1$ the maximal conversion is $f_{SQ}^{M2S} = \left|\mathrm{Cos}\left(\frac{\pi}{2(2k+1)}\right)\right|$ using $\bar{n}_1 = k$ echoes. By extending such argument to the case $2k < (\pi/\theta_1) < 2k+1$, it follows that a quasi-optimal choice of echoes is given by $\bar{n}_1(\varepsilon)$ in equation (4). The function $\bar{f}_{SQ}^{M2S}(\varepsilon) = f_{SQ}^{M2S}(\bar{n}_1)$ is plotted in figure S1.
The ZQ operator that follows the SQ block is

$$\rho_{ZQ_i} = \left(I_{1y}I_{2x}-I_{1x}I_{2y}\right)\mathrm{Sin}\, n_1\theta_1\,\mathrm{Cos}\, n_1\varphi_1 + \left(\frac{I_{1z}-I_{2z}}{2}\right)\mathrm{Sin}\, n_1\theta_1\,\mathrm{Sin}\, n_1\varphi_1 \quad S(9)$$

The free propagator generated by H_1 is a rotation in the ZQ space spanned by $\{ZQ_x = I_{1x}I_{2x} + I_{1y}I_{2y}, ZQ_y = I_{1y}I_{2x} - I_{1x}I_{2y}, ZQ_z = (I_{1z}-I_{2z})/2\}$. The blocks $[\pi-\tau]$ and $[\tau-\pi]$ are equivalent to rotations along the ZQ_y axis in the ZQ_{zx} plane by an angle $\theta_2 = -2\,\mathrm{ArcTan}(\varepsilon)$ and $\theta_2 = 2\,\mathrm{ArcTan}(\varepsilon)$, respectively.

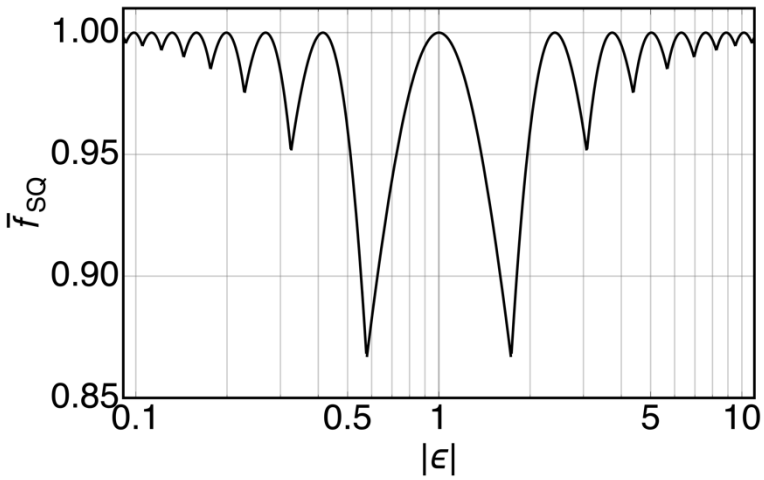

Fig. S1. The plot represents the M2S$_{SQ}$ transfer function $f_{SQ}^{\mathrm{M2S}}\left(\bar{n}_1\right)=\left|\mathrm{Sin}\,\bar{n}_1\theta_1\right|$, where $\overline{n_1}(\varepsilon)$ is given in Eq. 4. The cusps are at points $\theta_1 = \pi/(2k+1)$.

The aim of the M2S$_{ZQ}$ block is to maximize the projection along ZQ_x of the operator ZQ_i. This is achieved by selecting an appropriate delay to bring the initial zero-quantum operator from the zy plane into the zx plane and then to repeat n_2 times the block $[\pi - \tau]$ to drive the evolved operator as close as possible to the x axis. The orbit of the initial operator crosses the *zy* plane at delays $\bar{\Delta}_{\mp}$

$$\bar{\Delta}_{\mp}/\tau = \frac{1}{2} + \mathrm{Mod}\left[\mathrm{ArcTan}\frac{1}{\rho\mathrm{Tan}(\pi\bar{\mathrm{n}}_1\rho)}, \pi\right] \mp \frac{1}{2} \qquad S(10)$$

where $\rho = \frac{1}{(\sqrt{1+\varepsilon^2})}$ and then, periodically at timepoints multiple of 2τ. For each $\bar{\Delta}_{\mp}$, the transfer function for the transfer $ZQ_i \rightarrow ZQ_x$ is

$$f_{ZQ,\mp}^{M2S}(n_{2\mp}) = \left|\mathrm{Sin}\left[\left(\frac{1}{2}+n_{2\mp}\right)\theta_2 \mp \frac{|\mathrm{Sin}(\pi\bar{\mathrm{n}}_1\rho)|}{\sqrt{1+\frac{1}{\varepsilon^2}-\mathrm{Sin}^2(\pi\bar{\mathrm{n}}_1\rho)}}\right]\right| \qquad S(11)$$

In general, the optimal number of echoes is obtained by maximizing $f_{ZQ,\mp}^{M2S}$ as function of $n_{2\mp}$. Here, it was decided to take the minimum number of echoes $n_{2\mp}$ for which the full transfer function $\frac{I_{1x}+I_{2x}}{2} \rightarrow I_{1x}I_{2x} + I_{1y}I_{2y} + I_{1z}I_{2z} \rightarrow \frac{I_{1x}+I_{2x}}{2}$ was above 33%. The transfer function $f(\bar{n}_1, \bar{\Delta}_{\mp}, n_{2\mp})$ was computed using the SpinDynamica package (*41*). The number of echoes is given by

$$\bar{n}_{2-}(\varepsilon) = \begin{cases} \bar{n}_1(\varepsilon) - 1 & 0 < |\varepsilon| \le 0.4 \\ 1 & 0.4 < |\varepsilon| \le 0.7 \\ 0 & 0.7 < |\varepsilon| \le 2.5 \\ 1 & 2.5 < |\varepsilon| \le 2\pi \\ \mathrm{Round}\left[\frac{\varepsilon}{\pi}\right] & |\varepsilon| > 2\pi \end{cases} \qquad S(12)$$

$$\bar{n}_{2+}(\varepsilon) = \begin{cases} \bar{n}_1(\varepsilon) & 0 < |\varepsilon| \leq \sqrt{3} \\ \bar{n}_1(\varepsilon) + 1 & \sqrt{3} < |\varepsilon| \leq 2\pi \\ 2\bar{n}_1(\varepsilon) - \text{Round}\left[\frac{\varepsilon}{\pi}\right] & |\varepsilon| > 2\pi \end{cases} \qquad S(13)$$

The functions $\bar{\Delta}_{\mp}/\tau$, $\bar{n}_{2\mp}$ and $\bar{f}(\bar{n}_1, \bar{\Delta}_{\mp}, \bar{n}_{2\mp})$ are plotted in figure S2.

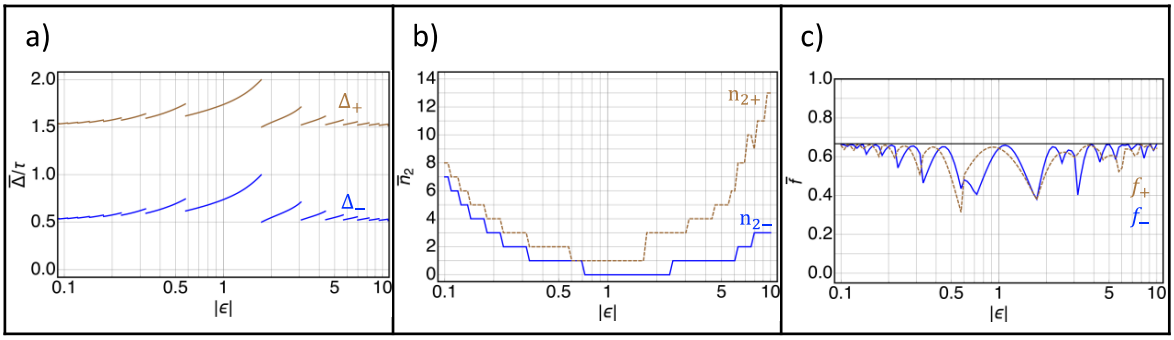

Fig. S2. Dependence of ε of the sequence parameters and transfer function. The ε dependences of the functions $\bar{\Delta}_{\mp}/\tau$, equation S9, $\bar{n}_{2\mp}$,equations S11 and S12 and $\bar{f}(\bar{n}_1, \bar{\Delta}_{\mp}, \bar{n}_{2\mp})$ are shown in panel a),b) and c), respectively. We would like to point out that c) shows the efficiency of the whole sequence meaning conversion of magnetization to singlet and back to magnetization.

Interestingly, the S2M block is not symmetric with respect to exchange of weak and strong coupling regime. In the limit of large ε, the number of echoes $\bar{n}_{2-} \cong 0.4\bar{n}_1$ represents a better choice as it is approximately ¼ of $\bar{n}_{2+}$. For such reason and for sake of simplicity, only the conditions $\bar{\Delta}_-$ and $\bar{n}_{2-}$ have been reported in the main section of the article. It is worth noting that in the intermediate region, higher efficiency can be reached for echoes $\bar{n}_{2\mp}$different to the reported values in exchange to a more complicated expressions for the dependency on ε.

In the singlet-to-magnetization section of the sequence, the ZQ_x component of the singlet state operator retraces backwards, closely but not exactly, the path discussed in the magnetization-to-singlet, according to

$$ZQ_x \xrightarrow{[\tau-\pi]^{\bar{n}_{2\mp}}-\left(\frac{\pi}{2}\right)_{\phi_3}} (I_{1x}I_{2z} - I_{1z}I_{2x})\,\text{Cos}\,\varphi_{S2M} + \left(\frac{I_{1y}-I_{2y}}{2}\right)\text{Sin}\,\varphi_{S2M} \xrightarrow{[\pi-\tau-\pi-\tau]^{\bar{n}_1}-\left(\frac{\pi}{2}\right)_{\phi_4}} \left(\frac{I_{1z}+I_{2z}}{2}\right). \qquad S(14)$$

This can be understood by the following observations: a) the ZQ echo block $[\tau-\pi]^{\bar{n}_{2\mp}}$ is a rotation of angle -$\bar{n}_{2\mp}\theta_2$ in the ZQ_{zx} plane; b) the delay $\bar{\Delta}_{\mp}$ create a ZQ_{zy} operator with phase $\varphi_{S2M} \cong -n_1\varphi_1$ opposite to that of the initial operator in the M2S$_{ZQ}$ block; c) the SQ echo block $[\pi-\tau-\pi-\tau]^{\bar{n}_1}$ corresponds to the transformation $R(-\bar{n}_1\theta_1)\otimes R(\bar{n}_1\varphi_1)$ that rewinds the final S2M state in the vicinity of the initial transverse state.

Simulations

The simulations of the spin dynamics of the sequence for a 2 spin system have been performed on a personal computer by a custom-built program ("notebook") based on the SpinDynamica packages developed from Levitt and coworkers (*41*) within the Wolfram Mathematica language (*42*).

The gc-M2S sequence was simulated using ideal delta-pulses with specified 90° and 180° flip angles. The phases of the relevant 90° flip pulse were set to $\phi_2 = x, \phi_3 = -x$. The phases of the 180° flip pulse were aligned along the x axis. The T$_{00}$-pass filter was simulated by projecting the incoming operator onto the 2-spin singlet operator $I_{1x}I_{2x} + I_{1y}I_{2y} + I_{1z}I_{2z}$. The initial operator in

all the simulation was set as $\rho_i = (I_{1x} + I_{2x})/2$. For the plot in figure S3, the spin system was set to $\delta_\nu = 3.4$ Hz and $J_{12} = 17$ Hz. The trajectories of the relevant single-quantum operators and zero-quantum-operators were followed in the corresponding SQ- and ZQ-blocks of the sequence. For the evaluation of the theoretical efficiency in figure S4c, the initial operator was propagated along the sequence using values $\bar{n}_1, \bar{\Delta}, \bar{n}_2$ from Equations (4), (5), (6) respectively. The reported efficiency f corresponds to the operator amplitude of the final operator over transverse magnetization operator $(I_{1x} + I_{2x})/2$.

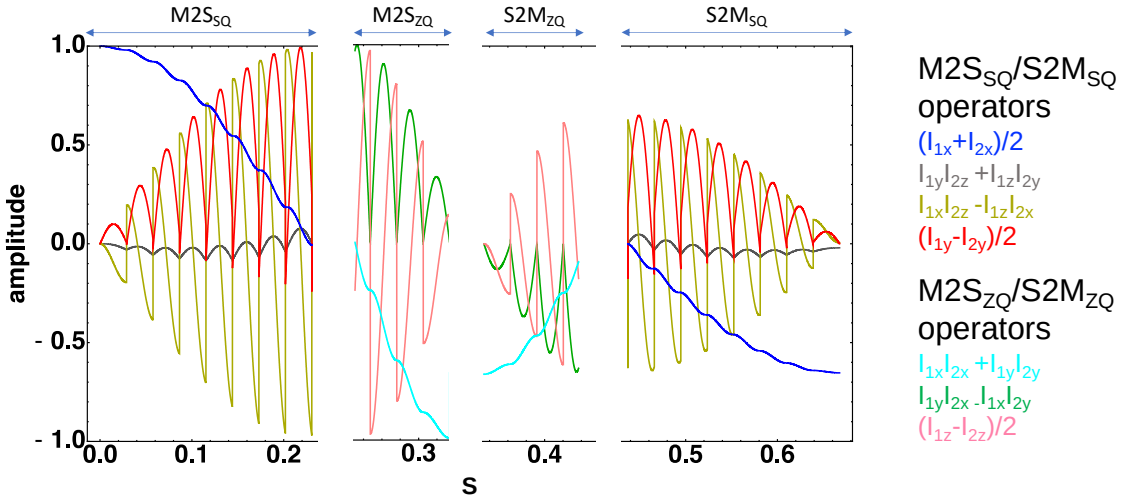

Fig. S3. The numerical simulation illustrates the spin dynamics during the core magnetization-to-singlet and singlet-to-magnetization blocks. In short, the first $(\pi/2)_{\phi_1}$ pulse brings longitudinal magnetization into the transverse plane. The core of the magnetization-to-singlet block converts magnetization (here transverse x-magnetization, 1st block, blue line) into zero quantum order $ZQ_x = I_{1x}I_{2x} + I_{1y}I_{2y}$ (2nd block, cyan line), which is projected into singlet order by the T_{00} filter. The S2M converts backwards ZQ_x (3rd block, cyan line) into magnetization (4th block, blue line).

Versatility and robustness

The gc-M2S sequence was applied on the tripeptide NH_2-Alanine-Glycine-Glycine-OH (AGG), which contains two sets of diastereotopic proton pairs at the α positions of the glycine residues G_1 and G_2. In each of these pairs, the protons are magnetically inequivalent to a different extent $\delta(H_\alpha)$=57.3ppb 12.6 ppb and $\delta(H_\alpha)$=12.6 ppb, respectively. The magnetic field was used to modify the ratio between the relative chemical shift and the *J*-couplings (~ 18Hz) in order to create different coupling regimes. For example, the weak, intermediate and strong coupled regimes were realized in AGG by performing experiments at 7.05T (300 MHz), 14.1T (600 MHz), 21.15 T (900 MHz) so that $|\varepsilon| = 1, 2, 3$ and $|\varepsilon| = 0.2, 0.4, 0.6$ and for G2 and G3, respectively. As shown in figure S4b-d, by using the gc-M2S parameters appropriate to the spin system of interest, it was possible to selectively convert magnetization into singlet order in each H_α pair of the glycine residues.

Next, 2,3-Dibromotiophene was studied as an example of the extremely weak coupling regime, with δ=0.37ppm and *J*=5.76Hz, so that $|\varepsilon|$ varies from 19 at 300 MHz to 38 at 600MHz and 57 at 900 MHz proton frequency. Interestingly, the gc-M2S sequence was able to convert magnetization into singlet and back to magnetization in the weakly coupled proton pairs even at such high $|\varepsilon|$ values (figure S4f-h).

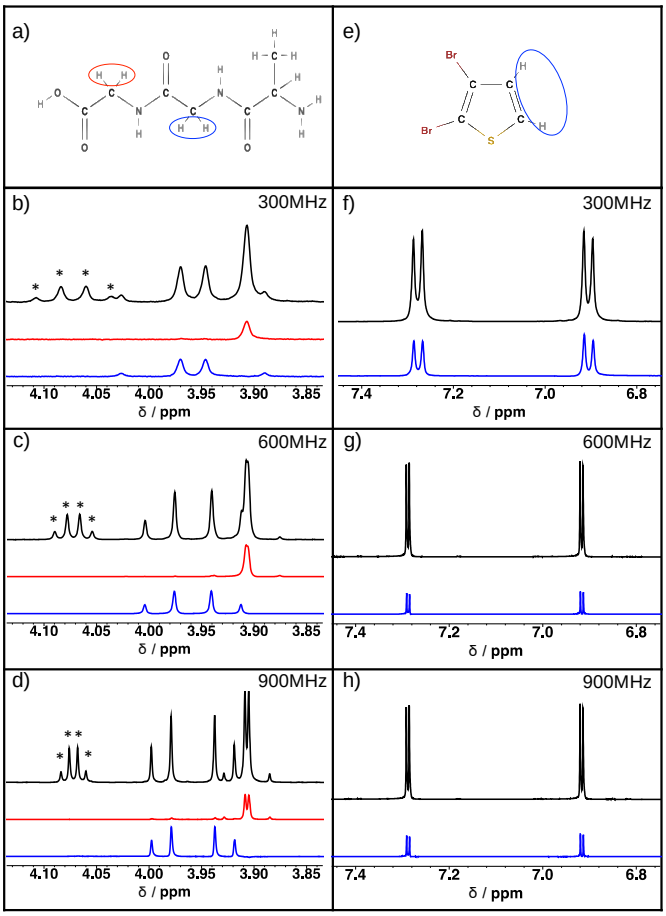

Fig. S4. NMR spectra and singlet filtering of model compounds at various magnetic fields. Panel a) shows the chemical structure of the AGG tripeptide. Panels b)-d) show from top to bottom the ^{1}H NMR spectra (black line) and singlet filtered spectra of AGG at the glcycine residue G2 (blue line) and G3 (red line) at three different fields corresponding to the ^{1}H Larmor frequency of 300MHz, 600MHz and 900MHz, respectively. The Hα alanine resonance, splitted by the coupling to the protons in the methyl chain, is denoted by *. Panel e) show the chemical structure of of 2,3-Dibromotiophene and panels f)-h) show from top to bottom the ^{1}H NMR spectra (black line) and singlet filtered at 300MHz, 600MHz and 900MHz, respectively. The spin Hamiltonian constants as well as the relevent experimental parameters are reported in SI.

As discussed in the theory section, assuming ideal delta-pulses, the offset Hamiltonian is irrelevant for magnetization-singlet conversion following the refocusing properties of the echoes and the general offset independence of the ZQ-evolution. For real finite-duration hard pulses, deviations from the nominal rotations as well as evolution during the pulses, have to be negligible for the sequence to work effectively. Figure S5 provides an experimental demonstration of the offset independence of the sequence for the Hα pairs of the two glycine residues in AGG. For each of the two pairs, the offset was systematically shifted off resonance from -4.5kHz to +4.5kHz in steps of 900Hz at 21.15T, which corresponds to a range of $\mp$5 ppm in 1 ppm steps. Within each set, the NMR signal remains in phase with variations of the integrated signal less than 20% across the explored range.

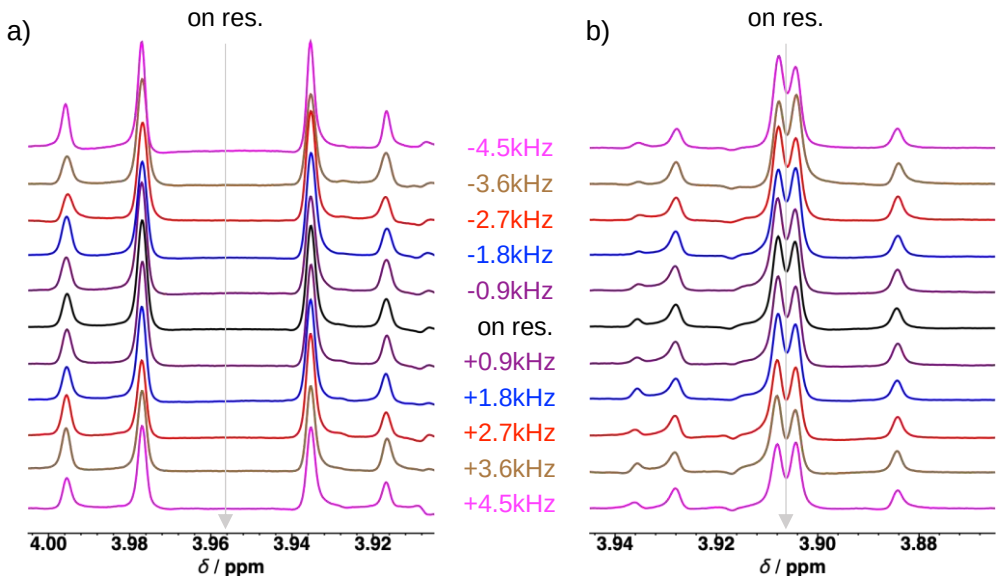

Fig. S5. The influence of the offset on the NMR signal passing through the gc-M2S sequence was evaluated in experiments on AGG at 21.15 T (900 MHz): panel a) residue G2 and panel b) residue G3. The grey lines represent the center of the multiplet for each residue, corresponding to the offset placed on exact resonance. From top to bottom, the offset was varied from minus to plus 4.5 kHz from the resonance in step of 900Hz. The experimental parameters for the sequence are the same as for figure S4, panel b)-d), see also table S1. The 90-degree flip pulse was ~10 μs.

^{1}H 1D NMR and ^{1}H-^{1}H TOCSY of Aβ40

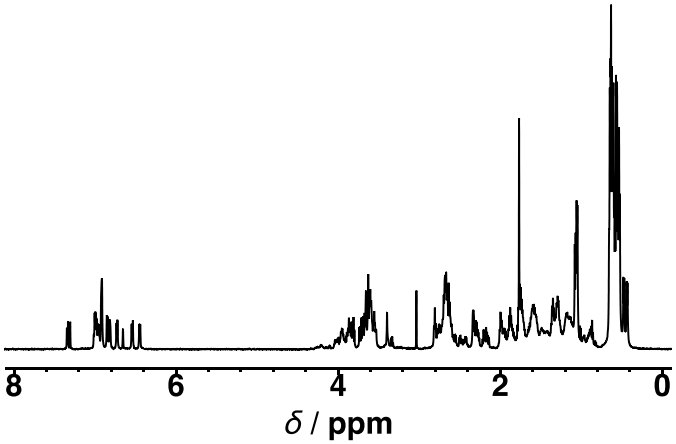

Fig. S6. ^{1}H NMR spectrum of Aβ40 in D_2O at 16.48 T (~700 MHz) and 278 K using a polynomial sequence for water suppression. Signal average of 64 scans.

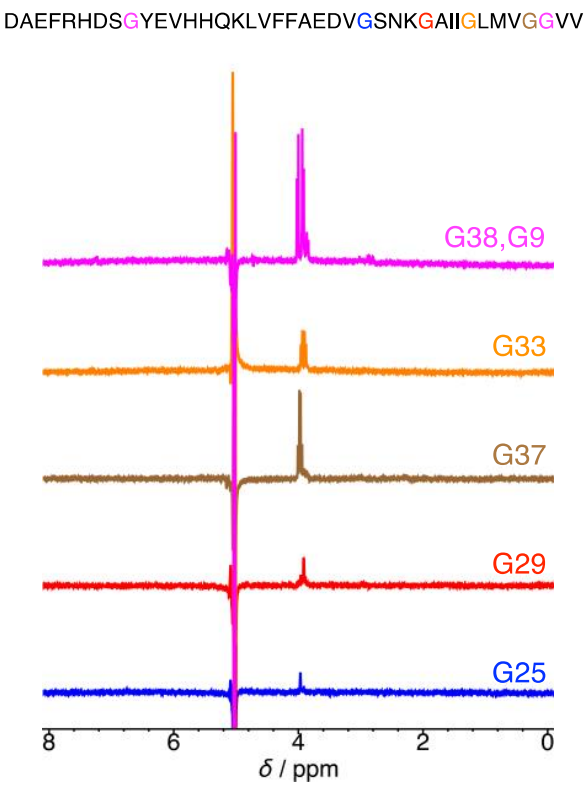

Fig. S7. ^{1}H NMR singlet-filtered spectra of Aβ40 in D_2O at 16.48 T (~700 MHz) and 278 K using the sequence of Fig. 1 with the parameters reported in table S3 to achieve selectivity for each glycine residue. Signal average of 512 scans.

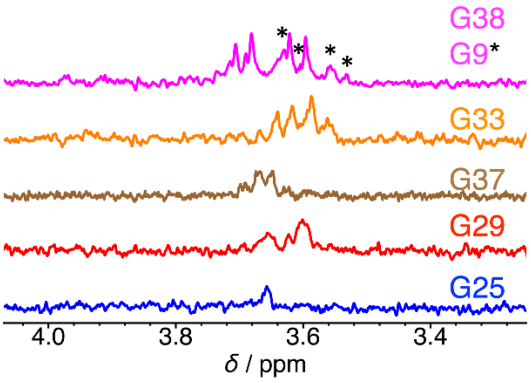

Fig. S8. ^{1}H NMR singlet-filtered spectra of Aβ40 in H_2O/D_2O (90%/10%) at 16.48 T (~700 MHz) and 278 K using the sequence of Fig. 1 with the parameters reported in table S3 to achieve selectivity for each glycine residue. Signal average of 2048 scans.

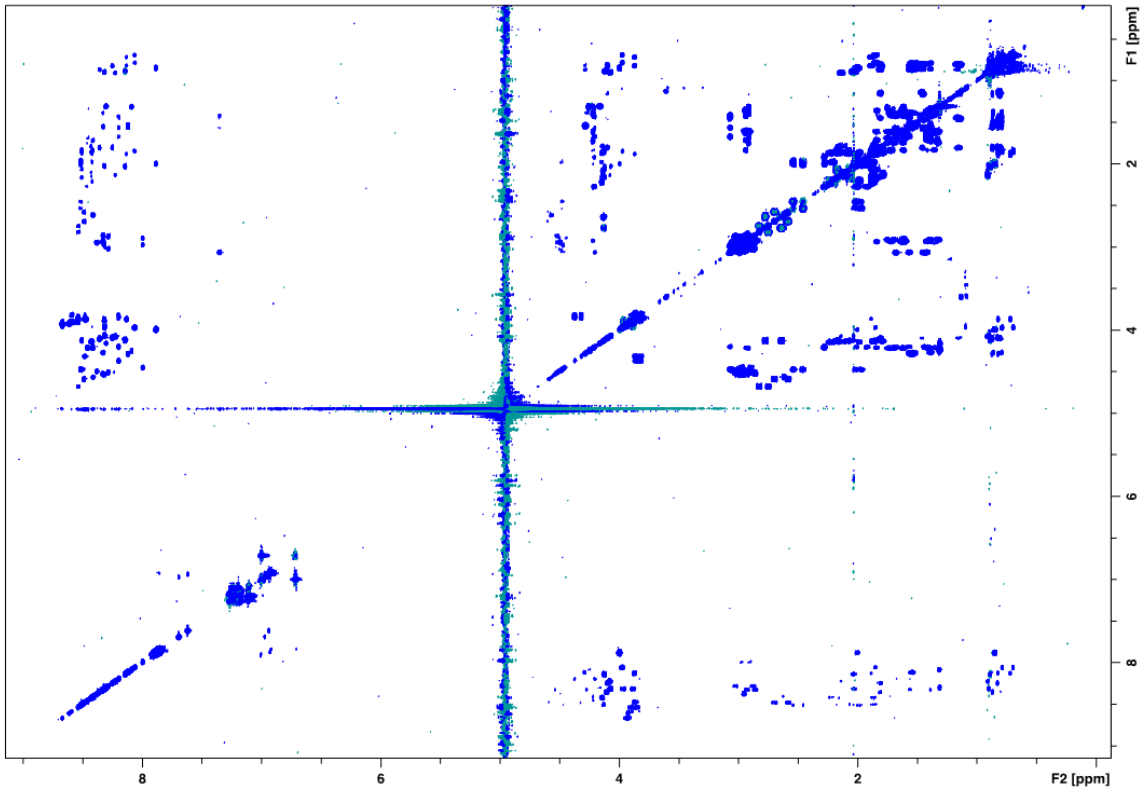

Fig. S9. TOCSY spectrum of Aβ40 in H_2O/D_2O (90%/10%) 16.48 T (~700 MHz) and 278 K obtained using a 60-ms DIPSI2 (ω_{RF} = 10 kHz) mixing block.

G29	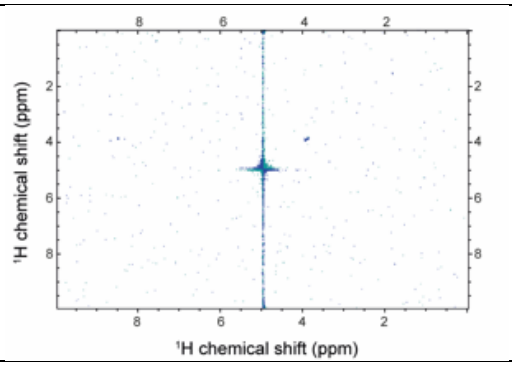
G33	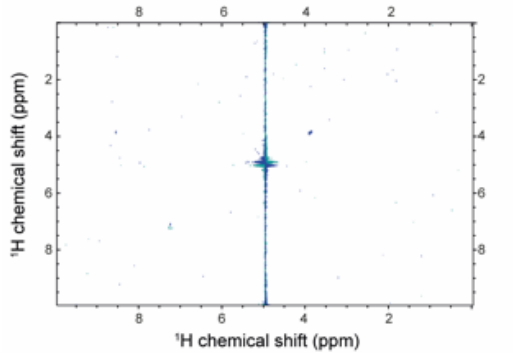
G37	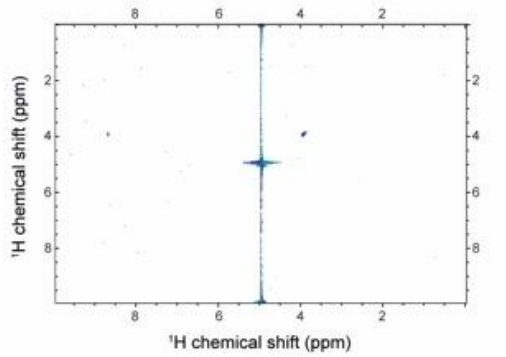
G38	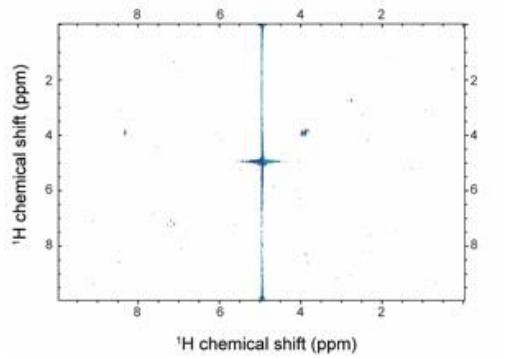

Fig. S10. Singlet-filtered TOCSYs spectra of Aβ40 in H_2O/D_2O (90%/10%) at 16.48 T (~700 MHz) and 278 K obtained using a 45-ms DIPSI2 (ω_{RF} = 10 kHz) mixing block. The singlet filtered sequence of Figure 1 was prepended to the TOCSY sequence using the parameters reported in table table S3 in order to achieve selectivity for the glycine residues at position 37 (left) and 38 (right), respectively.

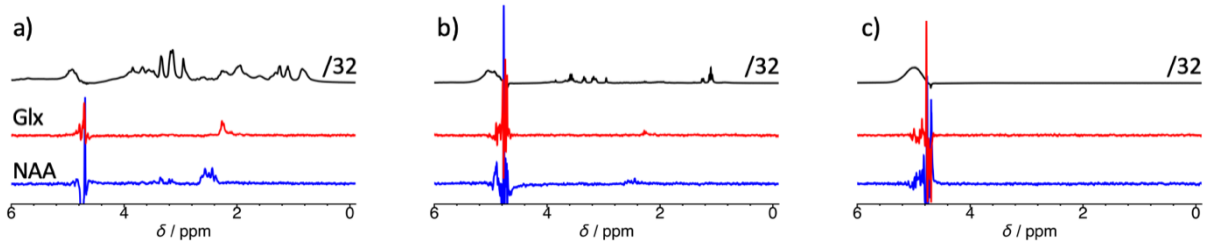

Fig. S11. Tissue control experiments. Experiments on (a) ex-vivo mouse cortices, (b) PBS buffer used from preserving the brains before insertion in the NMR tube (10 times more buffer volume was investigated than in (a)) and (c) PBS buffer only. In each panel the water suppressed spectrum (binomial suppression, zggpw5 Bruker library pulse program) is presented on top (black lines), scaled by a factor of 32 and singlet filtered experiments, matched for the H_γ pair of Glutamate (blue lines) and H_β pair (red lines) of NAA, are shown below. All experiments performed at 7.05T (300MHz) and 298K, using 3mL samples in 10 mm NMR tubes. The vertical scale is kept the same in all the 3 panels. The spectra in b) indicate minimal leaching of metabolites from the cortices in the buffer. The signal in a) comes therefore from the brain matter since the content of PBS in the cortex sample was less then 1/10th of the total volume used to record b).

Tables

The following tables collect the constants defining the nuclear spin Hamiltonian as well as the parameters used to set the gc-M2S sequence in the experiment presented in this article. $\delta_\nu = \omega_\delta/(2\pi)$ and J_{12} represent the chemical shift differences and the homonuclear *J*-couplings in the spin pairs of interest, respectively. ε is the ratio δ_ν/J_{12}. n_1 and n_2 represent the number of echoes for the single-quantum and the zero-quantum block of the gc-M2S sequence, respectively. τ represents the half-echo delay and Δ represents the zero-quantum delay. f_{exp} represents the experimental efficiency for the conversion of magnetization into singlet state and back to magnetization. It is calculated as the ratio between the integrated NMR signals obtained in the gc-M2S experiments and those obtained in the corresponding 90° pulse-acquire experiment. T_1 and T_s represent the characteristic relaxation times for the longitudinal magnetization and for the singlet state order to return to their thermal equilibrium values, respectively. T_1 were measured via standard inversion recovery experiments (180°-vd-90°-acquire, in which a variable delay vd is inserted between an inverting pulse and an acquiring pulse. T_s were measured by inserting a variable delay vd between the T_{00}-filter and the S2M block of the gc-M2S sequence, see Figure 1. For the duration of vd, the singlet was sustained by a RF-continuous wave with a nutation frequency between 3 and 10 times larger than the corresponding δ_ν. The integrated signals were fitted to a single exponential function $I(vd) = I_0 + I_1 e^{-vd/T}$ in order to extract the characteristic relaxation times.

Table S1. The table reports the constants defining the nuclear spin Hamiltonian as well as the parameters used to set the GE-M2S sequence in the experiments on the H_2N-AlanylGlycilGlycine-OH (AGG) peptide presented in figs. S4 (B to D) and S5. * indicates the spin constants that could not be extracted from the analysis of the ^1H NMR spectra. In such cases, the values from the resolved spectra at 900MHz were used for determining the sequence parameters.

12.8mM AGG in D_2O doped with 5μM Gd(III) , 298K											
Spectro-meter	Spin pair	Spin System parameters			gc-M2S parameters				gc-M2S	Relaxation times	
		$\lvert\delta_\nu\rvert$ / Hz	$\lvert J_{12}\rvert$ / Hz	$\lvert\varepsilon\rvert$	n_1	n_2	τ/ms	Δ/ms	f_{exp}	T_1/s	T_s/s
300 MHz	H_α(G2)	17.2	16.9	1.01	1	0	20.7	15.4	50%	0.83	14.3
	H_α(G3)	3.8*	18.0*	0.21	4	3	27.3	16.0	25%	0.92	6.0
600 MHz	H_α(G2)	34.3	16.9	2.03	2	0	13.1	7.2	50%	0.92	13.9
	H_α(G3)	7.6*	18.0	0.42	2	1	25.6	16.4	40%	1.05	5.7
900 MHz	H_α(G2)	51.6	16.9	3.04	2	1	9.2	6.5	50%	1.20	11.2
	H_α(G3)	11.4	18.0	0.63	1	1	23.6	15.0	40%	1.08	5.6

Table S2. The table reports the constants defining the nuclear spin Hamiltonian as well as the parameters used to set the gc-M2S sequence in the experiments on 2,3-dibromotiophene presented in fig. S4 (F to H).

2,3-Dibromotiophene in DCM/CDCl3 (1/40/10 v/v/v), 298K										
Spectro-meter	Spin System parameters			GEgc-M2S parameters				GEgc-M2S efficiency	Relaxation times	
	$\lvert\delta_\nu\rvert$ / Hz	$\lvert J_{12}\rvert$ / Hz	$\lvert\varepsilon\rvert$	n_1	n_2	τ/ms	Δ/ms	f_{exp}	T_1/s	T_s/s
300 MHz	111.5	5.76	19.4	15	6	4.5	2.3	40%	9.8	13.3
600 MHz	222.6	5.76	38.7	30	13	2.25	1.1	25%	10.3	15.1
900 MHz	334.5	5.76	58.1	46	20	1.49	0.75	25%	10.9	

Table S3. The table reports the constants defining the nuclear spin Hamiltonian as well as the parameters used to set the gc-M2S sequence in the experiments on Aβ40 presented in Fig. 2B. For H(G9), the calculated parameters are within round parentheses. The parameters for H(G25), labelled with a **, were experimentally optimized since δ_ν and J_{12} could not be determined from the NMR spectrum.

Aβ40 in D_2O, 278K (16.48T, 700MHz)							
Residue	Spin System parameters			gc-M2S parameters			
	$\lvert\delta_\nu\rvert$ / Hz	$\lvert J_{12}\rvert$ / Hz	$\lvert\varepsilon\rvert$	n_1	n_2	τ/ms	Δ/ms
H_α(G9)	55.0	17.2	3.2	3 (3)	0 (0)	8.2 (8.6)	4.5 (4.6)
H_α(G25)	--	--	--	1**	1**	25.5**	16**
H_α(G29)	14.8	16.7	0.9	1	0	22.5	15.8
H_α(G33)	38.1	16.7	2.28	2	0	12.0	7.0
H_α(G37)	24.6	16.9	1.46	1	0	16.8	14.9
H_α(G38)	58.4	16.9	3.45	3	0	8.2	4.5

Table S4. The table reports parameters used to set the gc-M2S sequence in the experiments on mouse brains presented in Fig. 3.

Brain Metabolites, 310K (7.05 T, 300MHz)				
Metabolite	gc-M2S parameters			
	n_1	n_2	τ/ms	Δ/ms
Glu/Gln	2	1	28.4	18
NAA	2	2	8.5	4

Materials and methods extended

For experiments described in SI, we used the following instruments and materials beside those reported in the main text.

Instrumentation

1. A 14.10 T (600 MHz ^{1}H Larmor frequency) superconducting magnet equipped with an inverse triple resonance cryo-probe (CPP TCI H&F-C/N-D-05 with Z gradient) and AVANCE-NEO console. Typical 90° pulse lengths were 7.5μs.
2. A 21.15 T (900 MHz ^{1}H Larmor frequency) superconducting magnet equipped with a triple resonance inverse cryo-probe (CP TCI 900S6 H-C/N-D-05) and AVANCE IIIHD console. Typical 90° pulse lengths were 10μs.

NH_2-AlanylGlycilGlycine-OH (AGG)

Boc protected AlanylGlycilGlycine-OH (Boc-AGG-OH) was bought from BACHEM and used without further purification. The protection group was removed by stirring a solution of Boc-AGG-OH in TFA (Trifluoro acetic acid) mixed with DCM (Dichloro methane) 50/50 v/v. The product was dried under active vacuum. The obtained powder was dissolved in D_2O to obtain a stock solution of H_2N-AlanylGlycilGlycine-OH (H_2N-AGG-OH). Gd(III) chloride hexahydrate ($GdCl_3 \cdot 6H2O$) was bought from Sigma Aldrich and a stock solution of Gd(III) in D_2O was prepared. A 12.8 mM solution of AGG with 5μM of Gd(III) in D2O was prepared by diluting the corresponding stock solutions. 500 μL of the final solution were transferred to a 5mm NMR tube for experiments.

2,3-Dibromotiophene

2,3-Dibromotiophene ($C_4H_2Br_2S$) was bought from Sigma Aldrich. A 1/60/10 (v/v/v) solution of dibromotiophene/dichloromethane/D-chloroform was prepared and 500 μL were transferred to a 5mm NMR tube for experiments.